freestream Reynolds number increases, less excitation would be required to produce the oscillation.

As the angle of attack is increased further, a higher frequency oscillation around 27 Hz is identified. This corresponds to a Strouhal number of 0.173 and is recognized as bluff body shedding. This frequency first became distinguishable at $\alpha=25$ deg and is clearly visible at 28 deg. The angle of attack when the bluff body shedding first occurred in the experiments of Zaman et al.[4] was much lower, about 18 deg, but their Reynolds number for the corresponding data was only 10^5.

Figure 3 presents the spectral intensities measured in the wake of the 12-in. chord aluminum model at several Reynolds numbers from 3×10^5 to 1.4×10^6. Here the spectra at $\alpha=14$ deg are shown, but the data at 15 deg are very similar. The frequency of the spectral peak is seen to increase with Reynolds number, although the Strouhal number remains nearly constant. Over the Reynolds number range shown, the magnitude of the peak appears to increase with Reynolds number. The spectra suggest that the low-frequency flow oscillation will continue to be present on this model at even higher Reynolds numbers.

A plot of Strouhal number vs Reynolds number for the present data and selected data from Ref. 4 are shown in Fig. 4. The present data taken at 15-deg angle of attack compare well to the earlier data[4] and seem to be a smooth extrapolation to the higher Reynolds numbers. Because of the magnitude of the forces induced by the flow oscillations and structural considerations, the wooden 10-in. chord model could only be used up to $Re=6\times10^5$. The 12-in. chord aluminum model was built to extend the data to the maximum tunnel speed and, therefore, Re, while still maintaining a low tunnel wall interference. Two trends are clearly seen in these data. The Strouhal number of the flow oscillation increases with model angle of attack and with increasing Reynolds number.

The increase in Strouhal number in these data is about 0.0034/10^6 Reynolds number. However, it should be noted that the phenomenon occurs over a small α range. Stepping in 1-deg increments in α, a clear peak in the u' spectra is only seen at $\alpha=14$ and 15 deg. Data from Ref. 4, shown in Fig. 4, also show a similar trend with angle of attack. The small increase in Strouhal number with Reynolds number seen in the present data was not apparent in the earlier data.[4]

Tunnel wall interference appears to affect the measured frequency of flow oscillation. Using exactly the same wooden 10-in. chord model, but in a much smaller tunnel, Zaman et al.[4] measured a Strouhal number of 0.033 at a Reynolds number of 3×10^5. The angle of attack at which the flow oscillation occurred was also higher at $\alpha=17$ deg. Considering only solid body and wake blockage, the increase in flow velocity at the model would only be about 5%,[7] not nearly enough to account for the discrepancy. An explanation of the discrepancy is not currently available.

Summary

A low-frequency flow oscillation on airfoils which occurs near the angle of maximum lift has been discussed. The frequency was measured with a hot-wire probe in the wake and was analyzed using a spectrum analyzer. Data available from Ref. 4 on a LRN(1)-1007 airfoil up to a Reynolds number of only 3×10^5 was extended to over 1.3×10^6. The frequency converts to a Strouhal number of approximately 0.02, which, from these data, appears to increase slightly with Reynolds number and more significantly with angle of attack.

References

[1]Zaman, K. B. M. Q., Bar-Sever, A., and Mangalam, S. M., "Effect of Acoustic Excitation on the Flow Over a Low-*Re* Airfoil," *Journal of Fluid Mechanics*, Vol. 182, 1987, pp. 127–148.

[2]Jones, B. M., "An Experimental Study of the Stalling of Wings," Aeronautical Research Committee Reports and Memoranda No. 1588, His Majesty's Stationery Office, London, Dec. 1933.

[3]Farren, W. S., "The Reaction on a Wing Whose Angle of Incidence is Changing Rapidly. Wind Tunnel Experiments With a Short Period Recording Balance," Aeronautical Research Committee Reports and Memoranda No. 1648, His Majesty's Stationery Office, London, Jan. 1935.

[4]Zaman, K. B. M. Q., McKinzie, D. J., and Rumsey, C. L., "A Natural Low-Frequency Oscillation of the Flow Over an Airfoil Near Stalling Conditions," *Journal of Fluid Mechanics*, Vol. 202, 1989, pp. 403–422.

[5]Bragg, M. B., and Khodadoust, A., "Experimental Measurements in a Large Separation Bubble Due to a Simulated Glaze Ice Accretion," AIAA Paper 88-0116, Jan. 1988.

[6]Reda, D. C., "Observations of Dynamic Stall Phenomena Using Liquid Crystal Coatings," *AIAA Journal*, Vol. 29, No. 2, 1991, pp. 308–310.

[7]Rae, W. H., and Pope, A., *Low-Speed Wind Tunnel Testing*, 2nd ed., Wiley, New York, 1984.

Mach Disk of Dual Coaxial Axisymmetric Jets

Anil K. Narayanan* and K. A. Damodaran†
Indian Institute of Technology, Madras, India

Nomenclature

D_i, D_m = diameter of the inner nozzle and Mach disk, respectively
P_a = ambient pressure
P_i, P_0 = inner and outer flow blowing pressures
X_m = axial location of Mach disk

Introduction

ONE of the distinctive features in the near-field shock wave structure of supersonic jets issuing from moderately/highly underexpanded nozzles is the normal shock or Mach disk existing in such flows. Extensive studies have already been carried out on Mach disk structure.[1–5] These studies are of importance in aerospace propulsion technology because sizable (in comparison to the nozzle exit diameter) Mach disks may appear in the flow issuing from nozzles of rocket/airbreathing engines when operating at very high altitudes or under highly underexpanded conditions. In the laboratory, such large sized Mach disks can be obtained only in high altitude test facilities using moderate to high pressure ratios.

Mach disks using two streams have been generated prior to this work,[6,7] but most of these studies have been confined to asymmetric Mach disks, generated by transverse injection of highly underexpanded flows into a supersonic stream. While conducting experiments on mixing of two coaxial axisymmetric, supersonic flows, the authors observed the existance of a large sized Mach disk even at relatively low pressure ratios across the main nozzle. Such a low pressure system of generating Mach disks should result in a simpler test setup compared to the existing high pressure, altitude simulation facilities. Therefore, some experiments were carried out to determine the effect of blowing pressures of the two streams on the size and location of the Mach disk. These experiments yielded some interesting results which are presented in this Note.

Description of Test Setup

The basic test setup shown in Fig. 1 was built to conduct studies on mixing of two high speed streams. It consisted of 1) an inner airstream with a convergent-divergent nozzle and 2) an outer, coaxial, annular airstream with a convergent nozzle. The outer stream makes an angle of about 26 deg with the axis of the inner stream. The inner nozzle was designed for a critical pressure ratio of 5:1. Both of the nozzles exit to the atmosphere. The diameter and axial location of the Mach disk was determined from shadowgraph of the freejet flowfield. Mach number was obtained from total and static pressure measurements along the axis.

Results

Shadowgraphs

Figure 2 shadowgraphs show that, for a constant value of P_i, as P_0 increases the Mach disk grows in size and shifts downstream.

Received Sept. 3, 1991; revision received Nov. 20, 1992; accepted for publication Nov. 27, 1992.

*Research Scholar, Aerospace Engineering Department.
†Professor, Aerospace Engineering Department.

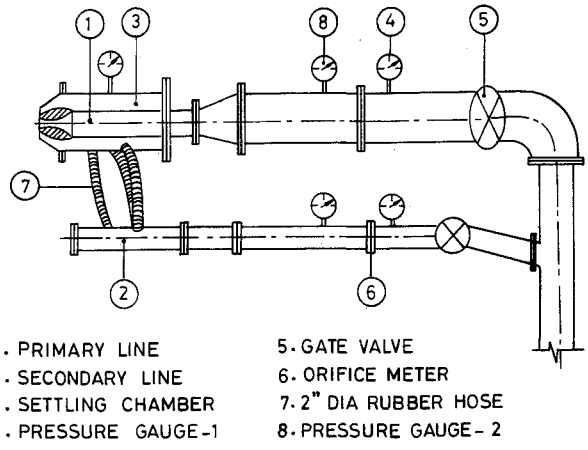

Fig. 1 Test setup.

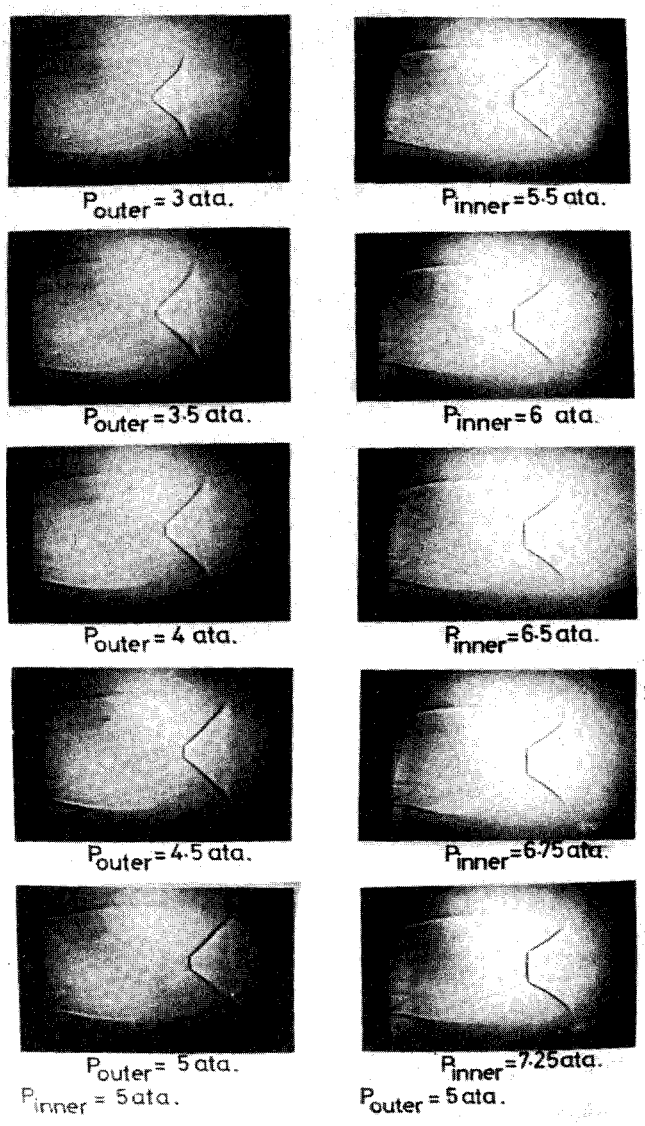

Fig. 2 Shadowgraphs.

Also, the absence of discrete shock waves in the inner flow at the nozzle exit indicates that the flow may have become subsonic due to the compression brought about by the outer flow. This was later verified by measurements of total and static pressures at the nozzle exit.

The photographs on the right bring out the effect of increasing P_i on the Mach disk keeping P_0 constant. Mach disk diameter is seen to increase considerably with increasing P_i. The subsonic region downstream of the Mach disk and the subsequent throat-like region can also be seen from these photographs.

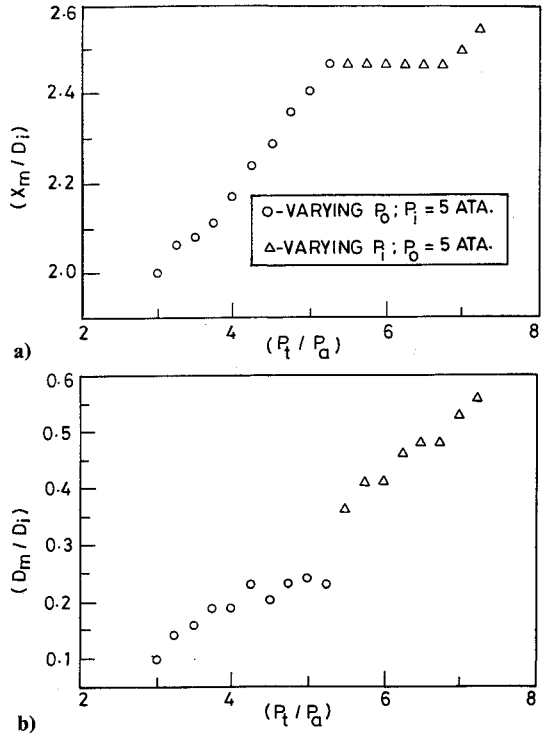

Fig. 3 Variation of Mach disk a) stand-off distance and b) diameter with blowing pressure.

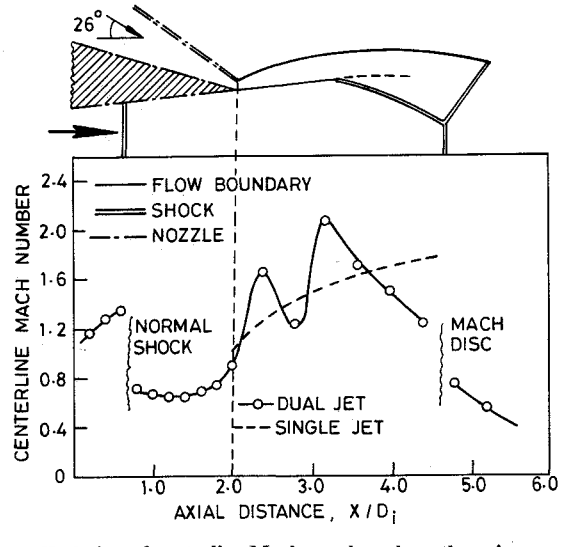

Fig. 4 Variation of centerline Mach number along the axis.

Mach Disk Geometry

Figure 3a shows the effect of stagnation pressure ratios P_0/P_a and P_i/P_a on axial location of the Mach disk X_m/D_i. X_m/D_i seems to increase linearly with P_0 or P_0/P_a. However, increasing P_i seems to have little effect on X_m except at relatively high values. Figure 3b shows a plot of D_m/D_i against P_i/P_a and P_0/P_a. As seen from these figures, increase in either P_i or P_0 results in a significant increase in D_m/D_i. Two major points to be noted from Fig. 3 are 1) empirical results based on earlier experimental data have shown that both X_m/D_i and X_m/D_i vary as square root of the stagnation pressure ratio for a single jet. However, results of the present study for the dual flow system indicate that they vary linearly with P_i; 2) with changes in P_0, X_m/D_i varies more or less linearly; but the D_m/D_i curve shows a maximum value at some optimum pressure ratio. The highest value of D_m/D_i obtained in these experiments was 0.56 for $P_i = 7.25$ atmospheres absolute and $P_0 = 5$ atmospheres absolute. An equivalent single jet would require a considerably higher blowing pressure to produce a Mach disk of similar size.

Centerline Mach Number

From total and static pressure measurements the centerline Mach numbers were calculated and plotted in Fig. 4 for $P_i = P_0 = 5$ ata. A normal shock is seen in the diverging section of the inner nozzle. Flow downstream of this shock is subsonic. Mach number decreases further up to about 20 mm from the nozzle exit. Farther downstream the flow accelerates up to the nozzle exit and beyond; perhaps due to flow separation in the diverging inner duct because of adverse pressure gradient and due to the presence of the outer flow impinging the inner flow at an angle. Superimposed on the axial Mach number distribution is a typical variation of centerline Mach number for a single, underexpanded, sonic jet. Figure 4 shows that the outer flow brings about a compression of the inner flow, creating a high static pressure zone near the exit of the inner nozzle similar to that of a highly underexpanded single flow. Injection angle of the outer flow may have a strong influence on the inner flow compression.

Conclusions

Conclusions that may be drawn from this limited experimental study are the following. 1) It is possible to obtain a sizable Mach disk ($D_m \sim D_i$) using a relatively low pressure test facility by employing dual, coaxial, axisymmetric jets; brought about by compression of the inner flow in the near zone by the outer flow. 2) With such an arrangement the Mach disk size varies linearly with P_i, whereas D_m/D_i variation with P_0 exhibits a maximum near $P_i = P_0$. 3) It is recognized that injection angle of the outer flow with respect to the inner may have a vital role in the Mach disk formation process. However, no tests were done varying the injection angle since the authors were primarily concerned with the study of the process of mixing of two coaxial high speed streams and not on the Mach disk formation process as such.

References

[1]Eastman, D. W., and Radtke, C. P., "Location of the Normal Shock Wave in the Exhaust Plume of a Jet," *AIAA Journal*, Vol. 1, No. 4, 1963, pp. 918, 919.

[2]Crist, S., Sherman, P. M., and Glass, D. R., "Study of the Highly Underexpanded Sonic Jet," *AIAA Journal*, Vol. 4, No. 1, 1966, pp. 68–71.

[3]Abbett, M., "The Mach Disk in Underexpanded Exhaust Plumes," *AIAA Journal*, Vol. 9, No. 3, 1971, pp. 512–514.

[4]Lewis, C. H., and Carlson, D. J., "Normal Shock Location in Underexpanded Gas and Gas-Particle Jets," *AIAA Journal*, Vol. 2, No. 4, 1964, pp. 776, 777.

[5]Bauer, A. B., "Normal Shock Location of Underexpanded Gas-Particle Jets," *AIAA Journal*, Vol. 3, No. 6, 1965, pp. 1187–1189.

[6]Zukoski, E. E., and Spaid, F. W., "Secondary Injection of Gases into a Supersonic Flow," *AIAA Journal*, Vol. 2, No. 10, 1964, pp. 1689–1696.

[7]Schetz, J. A., and Billig, F. S., "Penetration of Gaseous Jets Injected into a Supersonic Stream," *Journal of Spacecraft and Rockets*, Vol. 3, No. 11, 1966, pp. 1658–1665.

Front Body Effects on Drag and Flowfield of a Three-Dimensional Noncircular Cylinder

Khalid M. Sowoud* and E. Rathakrishnan†
Indian Institute of Technology, Kanpur 208 016, India

Introduction

THE subject of drag reduction is an interesting practical problem with a wide range of applications. Because of the difficulties associated with theoretical analysis, the study of drag reduction has been almost entirely experimental. At high enough Reynolds numbers the flow past a bluff body is characterized by a large wake zone. The separated shear layers from the sharp corners feed vorticity to the wake. These vorticies are shed continuously downstream. The side faces and the rear face are subjected to low pressure, whereas the front face is subjected to high positive pressure. With this flow pattern, the pressure drag coefficient assumes very large values (1.0–1.42). This fact is particularly true for bluff bodies with noncircular cross-sections and sharp corners.[5]

Several investigations deal with drag reduction of bluff bodies. Some of them directly relevant to the present study are Refs. 2–9.

In the present study the shielding effect of square-plate and D-shaped front bodies on the drag reduction and the pressure distribution of a three-dimensional bluff body is investigated.

Experimental Arrangement

The experiments were carried out in a $5.5 \times 3 \times 2$ ft low-speed, closed-circuit wind tunnel having a velocity range up to 45 m/s. The experimental model (Fig. 1) had three major parts. The rear body is a square box with windward sharp corners and rounded back with width $b_2 = 100$ mm, 108 mm long, and $R = 50$ mm. For the front body two shapes were used. The width of each front body varied from 0.25 to $1.0b_2$, and 12 different widths were tested. The gap between the front and rear bodies varied from 0.25 to $2.25b_2$, in steps of 0.25. The experiments were done for three speeds, which resulted in $Re_{b_2} = 1.0$, 1.4, and 1.8×10^5.

The drag force was measured directly using a three-component balance. For wall static pressure measurements the model was provided with 39 pressure taps, as shown in Fig. 1 (Sec. AA).

No blockage correction was done, since the configuration changes were not large, and all tests were made at zero angle of attack. At all runs, the blockage was only 1.79%.

Results and Discussion

For the basic body, the measured drag coefficients C_{D0} at the test Reynolds numbers based on rear-body width b_2 of 1.8, 1.4, and 1.0×10^5 were 1.42, 1.39, and 1.28, respectively. The high C_{D0} is mainly due to the positive pressure at the front face and the low pressure at the rear surface, as seen from Fig. 2. Of course, the skin friction also will contribute to the drag,

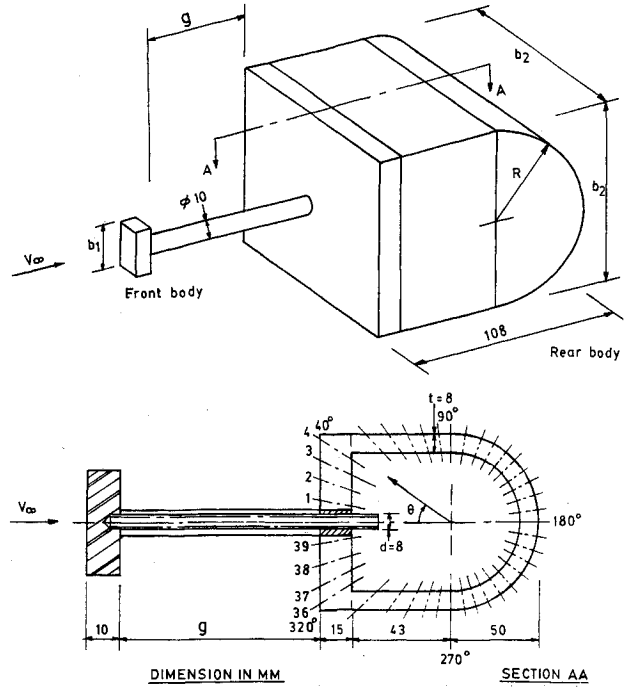

Fig. 1 Schematic diagram of the experimental model; in Sec. AA the numbers 1–39 refer to pressure tap locations.

Received March 9, 1992; revision received Oct. 12, 1992; accepted for publication Oct. 20, 1992.

*Graduate Student, Department of Aerospace Engineering.
†Associate Professor, Department of Aerospace Engineering.